Article

Not peer-reviewed version

Extracellular Matrix Disorganization at the Mesh–Tissue Interface in Chronic Surgical Mesh Rejection: A Multiscale Morphological Study

Adelina Tanevski [*] , Ludusanu Andreea [†] , Bogdan Mihnea Ciuntu [†] , Ștefan Lucian Toma [*] , Gheorghiță Balan , Raul-Vasile Lupusoru , Cristina Strobescu , Raluca Dragomir , Bogdan Florin Toma , Ciprian Gavrilă Ilea

Posted Date: 6 May 2026

doi: 10.20944/preprints202604.2206.v1

Keywords: chronic mesh rejection; atomic force microscopy; extracellular matrix; mesh–tissue interface; foreign body reaction

 doi:10.20944/preprints202604.2206.v1

Article

Extracellular Matrix Disorganization at the Mesh–Tissue Interface in Chronic Surgical Mesh Rejection: A Multiscale Morphological Study

Adelina Tanevski [1,*], Ludușanu Andreea [1,†], Bogdan Mihnea Ciuntu [1,†], Ștefan Lucian Toma [2,*], Gheorghiță Balan [1,†], Raul-Vasile Lupușoru [1], Cristina Strobescu [1], Raluca Dragomir [1], Bogdan Florin Toma [1] and Ciprian Gavrilă Ilea [1]

[1] Faculty of Medicine, Grigore T. Popa University of Medicine and Pharmacy, 700115 Iași, Romania

[2] Faculty of Materials Science and Engineering, Gheorghe Asachi Technical University of Iași, 700050 Iași, Romania

* Correspondence: stl_toma@yahoo.com (S.L.T.); papancea.adelina@umfiasi.ro (A.T.)

† These authors contributed equally to this work.

Abstract

Chronic surgical mesh rejection is a complex pathological process characterized by persistent inflammation, foreign body reaction, and progressive extracellular matrix (ECM) remodeling, leading to impaired tissue integration. Although histopathological features are well described, the structural organization of the ECM at the mesh–tissue interface remains insufficiently understood.This study aimed to investigate multiscale morphological alterations associated with chronic mesh rejection, with emphasis on ECM disorganization and loss of structural coherence. Seven mesh–tissue complexes explanted due to clinically confirmed chronic rejection were analyzed. Histological evaluation (hematoxylin–eosin and Van Gieson staining) was combined with atomic force microscopy (AFM), including topographical imaging, directional analysis, coherence mapping, and roughness quantification according to ISO 25178-2.Histology revealed chronic inflammatory infiltrates, foreign body reaction, and disorganized collagen deposition. AFM analysis showed pronounced surface heterogeneity, fragmented fibrillar architecture, and absence of preferential orientation. Roughness parameters (increased Sa and Sq, elevated Sku, negative Ssk) indicated a structurally irregular surface dominated by depressions and isolated peaks. Directional and coherence analyses confirmed loss of organized fibrillar architecture.These findings suggest that chronic mesh rejection is associated with marked ECM disorganization and loss of structural coherence at the mesh–tissue interface, reflecting impaired tissue integration. Multiscale morphological analysis provides insight into the structural basis of mesh failure and highlights the importance of ECM organization in implant–tissue interactions.

Keywords: chronic mesh rejection; atomic force microscopy; extracellular matrix; mesh–tissue interface; foreign body reaction

1. Introduction

The use of synthetic meshes has become a standard approach in the surgical repair of abdominal wall defects, significantly reducing recurrence rates and improving long-term outcomes [1]. However, mesh implantation is associated with a range of complications, among which chronic mesh rejection represents a particularly challenging clinical condition. It is commonly characterized by persistent pain, local inflammation, and functional impairment of the abdominal wall, often requiring surgical explantation of the prosthetic material [2].

From a biological perspective, mesh rejection is not a single event but a sustained process driven by chronic inflammation and foreign body reaction [3]. Following implantation, host tissue

 doi:10.20944/preprints202604.2206.v1

undergoes dynamic remodeling involving immune cell infiltration, fibroblast activation, and progressive extracellular matrix (ECM) reorganization. While these processes may support functional integration under favorable conditions, persistent inflammatory stimuli can promote pathological remodeling, resulting in fibrosis, structural disorganization, and impaired tissue–implant interaction [4,5].

The extracellular matrix plays a central role in maintaining tissue architecture and mechanical integrity. Under normal conditions, collagen fibers exhibit a structured and anisotropic organization, enabling efficient load distribution and coordinated mechanical behavior [6]. In contrast, chronic inflammatory environments are associated with altered collagen deposition, loss of fibrillar alignment, and increased structural heterogeneity [7], changes that may compromise ECM coherence and functional integration of implanted biomaterials [8].

Despite well-recognized histopathological features of mesh rejection, the structural organization of the ECM at the mesh–tissue interface remains insufficiently characterized, particularly at the nanoscale. Conventional histological techniques provide valuable qualitative information but are limited in capturing fine structural details and spatial organization of fibrillar components [9]. In this context, atomic force microscopy (AFM) enables high-resolution investigation of surface topography, fibrillar orientation, and structural heterogeneity [10].

Therefore, the aim of this study was to investigate multiscale morphological alterations associated with chronic surgical mesh rejection, with a focus on ECM disorganization and loss of structural coherence at the mesh–tissue interface. By integrating histological assessment with nanoscale analysis, this study aims to provide a more comprehensive understanding of the structural basis of impaired tissue integration.

2. Materials and Methods

2.1. Study Design and Sample Collection

This study was designed as a descriptive experimental investigation aimed at characterizing the morphological and nanostructural features of the mesh–tissue interface in chronic surgical mesh rejection.

A total of seven mesh–tissue complexes were analyzed, each obtained from a different patient undergoing surgical explantation due to clinically and intraoperatively confirmed chronic mesh rejection. All patients presented persistent symptoms, including chronic pain, local inflammation, and functional impairment of the abdominal wall, requiring mesh removal.

Only specimens containing both prosthetic material and adherent fibro-inflammatory tissue were included. Patients with uncontrolled systemic infection, extensive tissue necrosis compromising structural assessment, or ongoing major immunomodulatory therapy were excluded. All patients provided informed consent for the use of surgical specimens for research purposes.

2.2. Tissue Sampling and Processing

Specimens were collected intraoperatively using standard surgical techniques, without altering the clinical procedure. Tissue fragments were obtained from areas macroscopically characterized by fibrotic thickening, chronic inflammatory changes, and foreign body reaction.

To preserve structural integrity, samples were excised using cold instruments, avoiding thermal damage. Each specimen had an approximate thickness of 0.5 mm to ensure consistency across samples.

Immediately after collection, samples were stabilized in RNAlater® solution to minimize post-excision degradation. Prior to analysis, specimens were rinsed in DPBS (1×, pH 7.0) to remove residual storage medium and provide a standardized buffered environment.

 doi:10.20944/preprints202604.2206.v1

2.3. Histological Analysis

Tissue fragments designated for histological examination were fixed in buffered formalin, processed using standard techniques, paraffin-embedded, and sectioned at conventional thickness.

Sections were stained with hematoxylin–eosin (H&E) to assess general tissue morphology, cellular distribution, and inflammatory infiltrates, and with Van Gieson (VG) staining to evaluate collagen organization and extracellular matrix architecture.

Histological analysis was performed qualitatively, focusing on chronic inflammatory changes, fibrosis patterns, and alterations in collagen organization associated with mesh rejection.

2.4. Afm Sample Preparation

For atomic force microscopy analysis, tissue fragments were mounted on poly-L-lysine-coated glass slides to ensure adequate adhesion and mechanical stability during scanning.

All measurements were performed in air at room temperature (approximately 22–24 °C), on samples analyzed shortly after collection to preserve native structural features.

2.5. Afm Imaging and Morphological Analysis

Nanoscale morphological characterization was performed using an EasyScan 2 atomic force microscope (Nanosurf AG, Liestal, Switzerland), equipped with the manufacturer's acquisition and analysis software.

Topographical imaging was conducted in contact mode using PPP–NCSTAuD probes (Nanosensors, Neuchâtel, Switzerland), featuring a conical tip with a nominal radius below 7 nm. Scans were acquired over standardized areas of 2 × 2 μm², and multiple regions of interest were analyzed for each specimen to account for local structural heterogeneity.

Raw AFM data were processed using plane leveling (Least Squares Plane Leveling, LSPL), followed by application of a Gaussian L-filter with a cutoff wavelength (λc) of 0.8 μm to remove long-wavelength components associated with global surface form.

2.6. Surface Roughness Analysis

Areal surface roughness parameters were calculated in accordance with ISO 25178-2 standards, including Sa (arithmetical mean height), Sq (root mean square height), Ssk (skewness), Sku (kurtosis), Sp (maximum peak height), Sv (maximum pit depth), and Sz (maximum height).

These parameters were used to quantitatively characterize surface heterogeneity and structural irregularities associated with pathological extracellular matrix remodeling.

2.7. Directionality and Coherence Analysis

The spatial organization of surface structures was evaluated through directional analysis of AFM topography data, assessing the presence or absence of preferential fibrillar orientation.

Coherence mapping was used to quantify the local consistency of structural orientation, providing insight into the degree of spatial organization and fragmentation of the fibrillar architecture.

Together, these analyses enabled the assessment of structural anisotropy and the identification of alterations associated with pathological extracellular matrix remodeling.

2.8. Data Analysis

Data analysis was performed using a descriptive approach aimed at identifying recurrent morphological patterns across samples. Multiple regions of interest were analyzed for each specimen to capture local structural variability.

Given the exploratory nature of the study and the limited sample size, no inferential statistical analysis was performed.

 doi:10.20944/preprints202604.2206.v1

3. Results

3.1. Histological Findings

Van Gieson staining (×10) revealed a dense chronic inflammatory infiltrate with increased cellularity, including numerous macrophages, some exhibiting foamy cytoplasm, and multinucleated giant cells within the fibro-inflammatory tissue adherent to the prosthetic material (**Figure 1**). The extracellular matrix appeared markedly disorganized, with fragmented and irregularly arranged collagen fibers and loss of normal fibrillar architecture.

Areas consistent with foreign body reaction were observed, supporting the presence of persistent pathological remodeling at the mesh–tissue interface. Overall, these findings are consistent with advanced extracellular matrix disruption and impaired tissue integration in chronic mesh rejection.

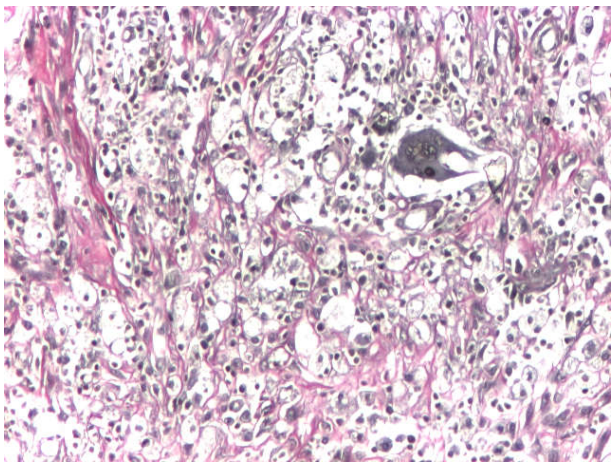

Figure 1. Histological features of the mesh–tissue interface in chronic surgical mesh rejection. Van Gieson staining (×10) showing disorganized collagen architecture with fragmented and irregularly arranged fibers, associated with a dense inflammatory infiltrate including multinucleated giant cells and macrophages (some with foamy cytoplasm). Features of foreign body reaction are present.

Van Gieson staining (×10) revealed extensive alterations in collagen organization at the mesh–tissue interface (**Figure 2**). The normal fascicular architecture was absent and replaced by irregularly distributed, fragmented collagen fibers.

Collagen bundles appeared thickened, intersecting, and lacking coherent orientation. Areas of increased cellularity associated with inflammatory infiltrates and reactive fibroblasts were also observed.

Overall, these features are consistent with disorganized fibrotic deposition and loss of extracellular matrix structural coherence in chronic mesh rejection.

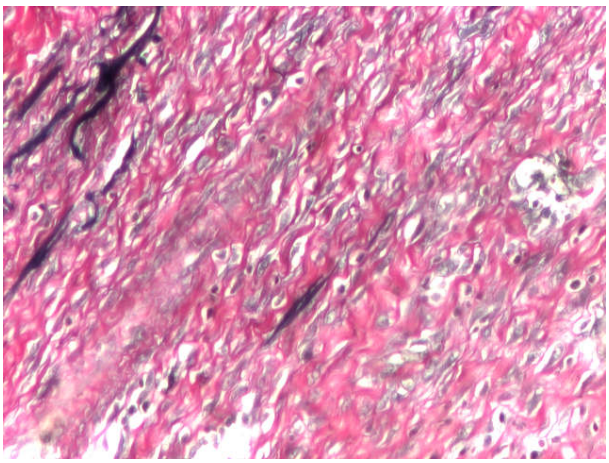

 doi:10.20944/preprints202604.2206.v1

Figure 2. Histological features of extracellular matrix remodeling at the mesh–tissue interface in chronic surgical mesh rejection. Van Gieson staining (×10) demonstrating marked disorganization of collagen fibers, with irregular distribution, fragmentation, and loss of normal fibrillar architecture. Areas of increased cellularity and fibro-inflammatory changes are present, consistent with pathological extracellular matrix remodeling.

3.2. Afm Nanostructural Characterization

AFM deflection imaging, acquired in forward scanning mode over a 2 × 2 μm² area, reflects local variations in tip–sample interaction forces, including contributions from surface stiffness, adhesion, and friction, without directly representing geometric topography (**Figure 3**).

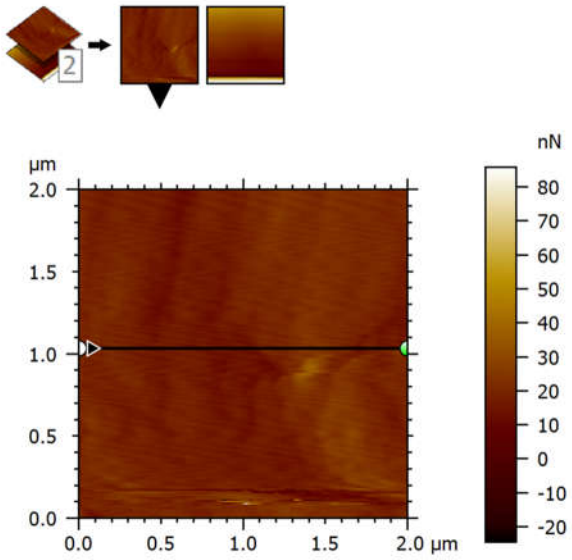

Figure 3. AFM deflection map (forward scan) showing pronounced structural heterogeneity and loss of collagen fibrillar organization at the mesh–tissue interface in chronic surgical mesh rejection.

The deflection map revealed pronounced submicron-scale structural heterogeneity at the mesh–tissue interface in chronic mesh rejection, with alternating regions of low and high deflection corresponding to local variations in the tip–sample interaction signal.

Fibrillar structures appeared disorganized, lacking preferential orientation and exhibiting a fragmented and intersecting pattern. Localized domains of increased deflection were observed and may correspond to dense inflammatory tissue, fibrin deposition, or altered mechanical coupling between tissue and residual prosthetic elements.

The absence of major scanning artifacts supports stable tip–sample interaction and the reliability of the acquired data.

AFM topography (forward scan) demonstrated pronounced surface heterogeneity, with irregularly distributed height variations across the analyzed area (Figure 4). The lack of coherent fibrillar architecture and lamellar organization is consistent with severe collagen disorganization.

Fibrillar structures appeared fragmented and irregularly arranged, with prominent localized elevations ranging from submicron to micrometric scales. These features may correspond to fibro-inflammatory accumulations, granulation tissue, or immature extracellular matrix deposition associated with chronic remodeling.

A relatively uniform linear feature observed at the lower margin of the image was interpreted as a scanning artifact or boundary effect and was excluded from quantitative analysis.

Overall, AFM topography indicates extensive structural remodeling, characterized by loss of continuity and disruption of organized collagen architecture.

 doi:10.20944/preprints202604.2206.v1

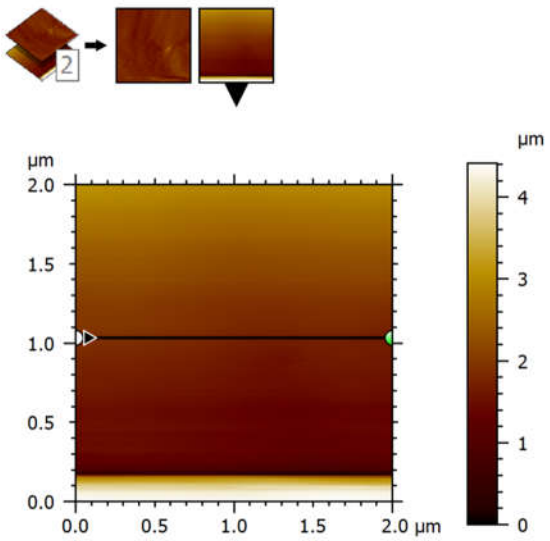

Figure 4. AFM topography (forward scan) showing pronounced morphological heterogeneity and pathological remodeling at the mesh–tissue interface in chronic surgical mesh rejection.

Three-dimensional AFM reconstruction revealed a highly irregular surface morphology, with height variations reaching several hundred nanometers (**Figure 5**). The surface was characterized by steep gradients, discontinuities, and lack of structural coherence.

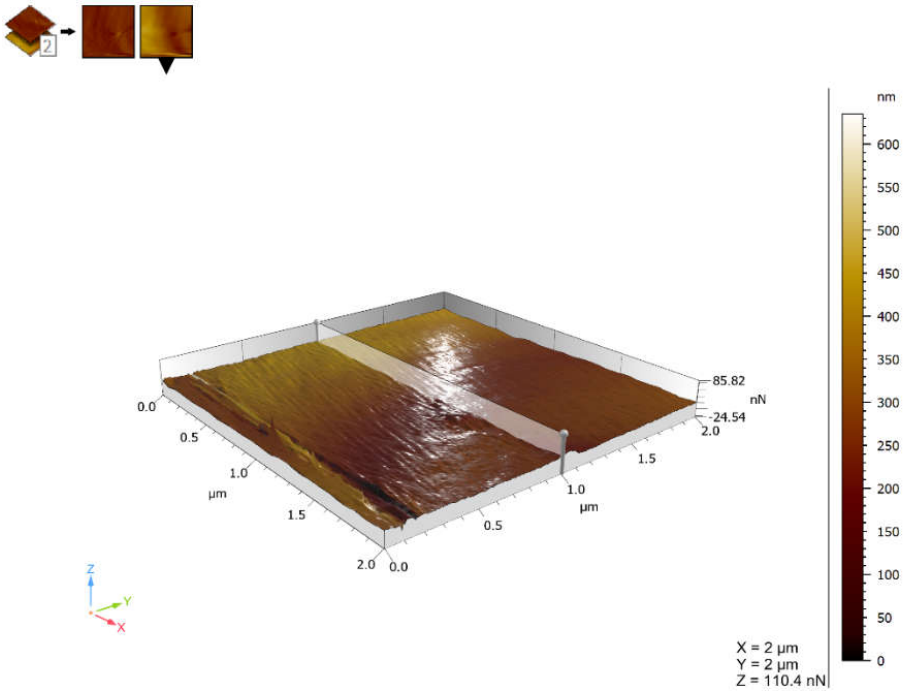

Figure 5. Three-dimensional AFM topography of the mesh–tissue interface illustrating pronounced surface irregularity and structural disorganization in chronic surgical mesh rejection.

Unlike the relatively ordered architecture observed in integrated tissue, the analyzed surface exhibited prominent elevations and deep depressions distributed without a consistent spatial pattern. These features are consistent with disrupted extracellular matrix organization and ongoing pathological remodeling.

Localized elevated domains, ranging from submicron to micrometric dimensions, were observed and may correspond to fibro-inflammatory deposits, granulation tissue, or areas of immature matrix accumulation.

 doi:10.20944/preprints202604.2206.v1

Spatial anisotropy was limited to local regions and lacked global coherence, indicating fragmented structural organization.

Overall, the three-dimensional morphology suggests that the mesh–tissue interface behaves as a structurally discontinuous system composed of heterogeneous domains rather than a cohesive biomechanical unit.

3.3. Surface Roughness and Profile Analysis

Areal surface roughness was quantified according to ISO 25178-2 using a Gaussian L-filter (λc = 0.8 μm), without application of an S-filter, enabling characterization of the intrinsic micro- and mesostructural features of the surface (**Table 1**).

Table 1. Areal surface roughness parameters of the mesh–tissue interface in chronic surgical mesh rejection, determined by atomic force microscopy (AFM) in accordance with ISO 25178-2.

Parameter	Description	Value	Unit
Sa	Arithmetical mean height	13.86	nm
Sq	Root mean square height	28.35	nm
Ssk	Skewness of height distribution	−0.2197	–
Sku	Kurtosis of height distribution	31.22	–
Sp	Maximum peak height	304.9	nm
Sv	Maximum pit (valley) depth	286.5	nm
Sz	Maximum height (peak-to-valley)	591.3	nm

The arithmetical mean height (Sa = 13.86 nm) and root mean square height (Sq = 28.35 nm) indicate a moderately to highly rough surface with increased variability in local height distribution, reflecting pronounced surface heterogeneity.

Negative skewness (Ssk = −0.2197) suggests a surface dominated by depressions, consistent with localized extracellular matrix collapse. The markedly elevated kurtosis (Sku = 31.22), well above the Gaussian reference value (Sku = 3), indicates the presence of isolated high peaks on an otherwise irregular surface.

The comparable values of Sp (304.9 nm) and Sv (286.5 nm), together with the large peak-to-valley height (Sz = 591.3 nm), further support the presence of pronounced surface irregularities.

Overall, these roughness parameters are consistent with a highly heterogeneous and structurally disorganized surface associated with chronic mesh rejection.

The surface profile extracted from the central region (**Figure 6**) further illustrates this heterogeneity, showing height variations ranging from approximately +120 nm to −100 nm over a length of ~2 μm.

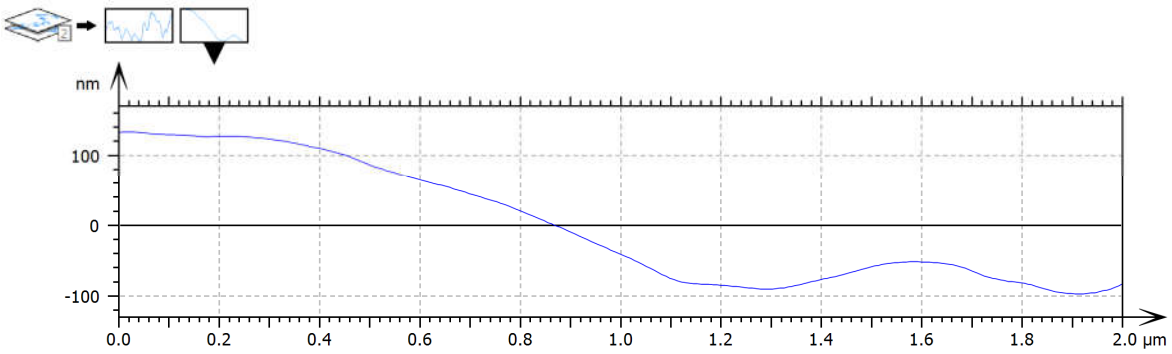

 doi:10.20944/preprints202604.2206.v1

Figure 6. AFM surface profile of aponeurotic tissue associated with chronic surgical mesh rejection.

The surface profile showed an irregular morphology with abrupt transitions between local maxima and minima, indicating pronounced geometric disorganization.

In the initial segment (0–~1.0 μm), a marked gradient was observed, with a progressive height decrease exceeding 200 nm, reflecting structural unevenness of the aponeurotic surface. Around the central region (~0.9–1.1 μm), an abrupt transition from positive to negative height values suggests a boundary between structurally distinct domains.

In the remaining segment (1.1–2.0 μm), the profile exhibited irregular oscillations with height variations of approximately 30–60 nm and non-uniform spatial frequency, consistent with disorganized collagen fibrils.

These observations are in agreement with the areal roughness parameters (high Sku, negative Ssk, large Sz), supporting the presence of a heterogeneous and structurally fragmented surface.

Overall, the surface profile suggests a discontinuous organization of the aponeurotic surface into distinct structural domains, consistent with incomplete tissue integration in chronic mesh rejection.

3.4. Directionality and Structural Organization

The directional distribution of surface orientations derived from AFM topography is shown as a polar histogram (**Figure 7**). It reflects the local orientation of ridges, fibrillar elements, and morphological discontinuities, allowing assessment of preferential structural alignment at the mesh–tissue interface.

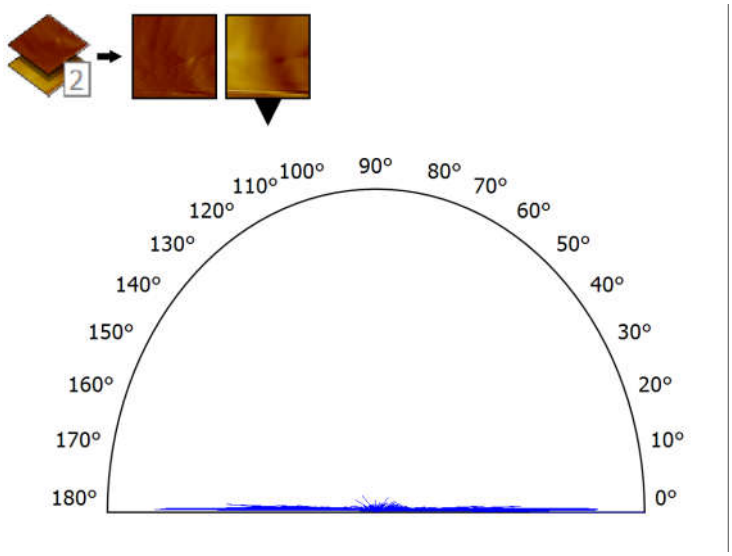

Figure 7. Directional distribution of surface structural orientations derived from AFM topography at the mesh–tissue interface in chronic surgical mesh rejection.

The polar histogram shows an almost uniform distribution without distinct directional peaks, indicating the absence of a coherent preferential orientation. The identified principal directions (≈0°, ≈175°, and ≈5°) are closely grouped and do not define a dominant axis, supporting a near-random distribution of structural orientations.

In contrast, favorably integrated tissue typically exhibits anisotropic organization with one or two dominant directions corresponding to aligned collagen fibers. The near-isotropic distribution observed here reflects loss of directional architecture at the mesh–tissue interface.

This pattern suggests disorganized tissue remodeling associated with chronic fibro-inflammatory processes and impaired structural integration.

Consistent findings were observed in the directional analysis derived from AFM topography (**Figure 8**), which also lacked clearly defined dominant orientations.

 doi:10.20944/preprints202604.2206.v1

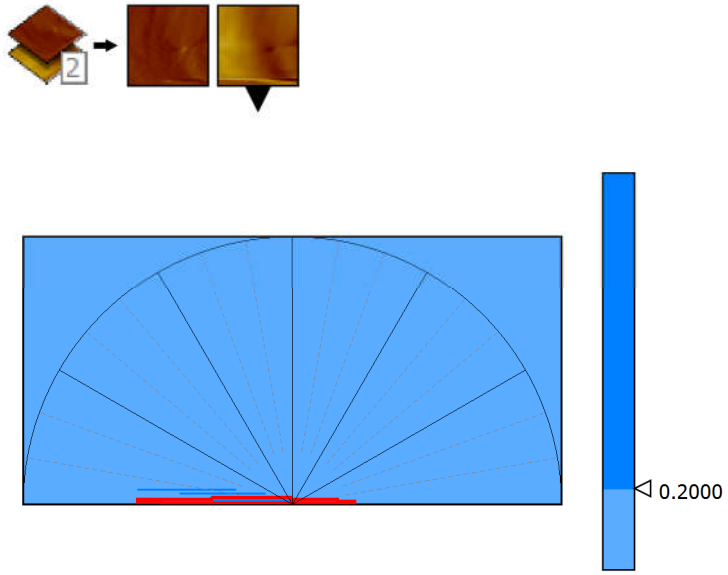

Figure 8. Directional distribution of surface structures derived from AFM topography at the mesh–tissue interface in chronic surgical mesh rejection.

Importantly, this analysis is based exclusively on the AFM topography channel, which reflects the true geometric surface morphology, rather than the deflection signal. Therefore, the observed directional distribution represents a purely morphological characterization, independent of local mechanical response.

Advanced topographical analysis, integrating directional texture, height distribution, and bearing capacity, is presented in **Figure 9**. Directional texture analysis revealed no clear periodicity or dominant orientation, indicating loss of organized fibrillar architecture.

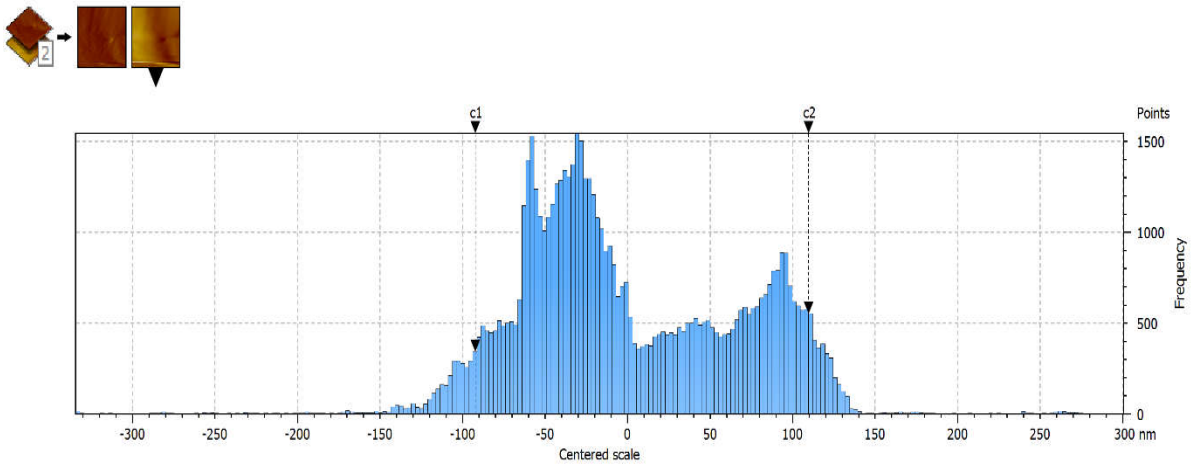

Figure 9. Advanced topographical characterization of the mesh–tissue interface derived from AFM topography, including directional texture analysis, height distribution histogram, and Abbott–Firestone curve in chronic surgical mesh rejection.

The height distribution histogram showed a broad and asymmetric profile, indicating pronounced surface heterogeneity with coexisting elevated regions and deep depressions.

The Abbott–Firestone curve demonstrated a non-uniform material distribution with depth. The steep slope in the central region suggests that mechanical support is likely distributed across isolated structural domains rather than a continuous matrix.

 doi:10.20944/preprints202604.2206.v1

The spatial distribution of coherence values (**Figure 10**) further supports this finding, with a spectrum dominated by low values, indicating weak spatial correlation of fibrillar orientations and absence of sustained directional organization.

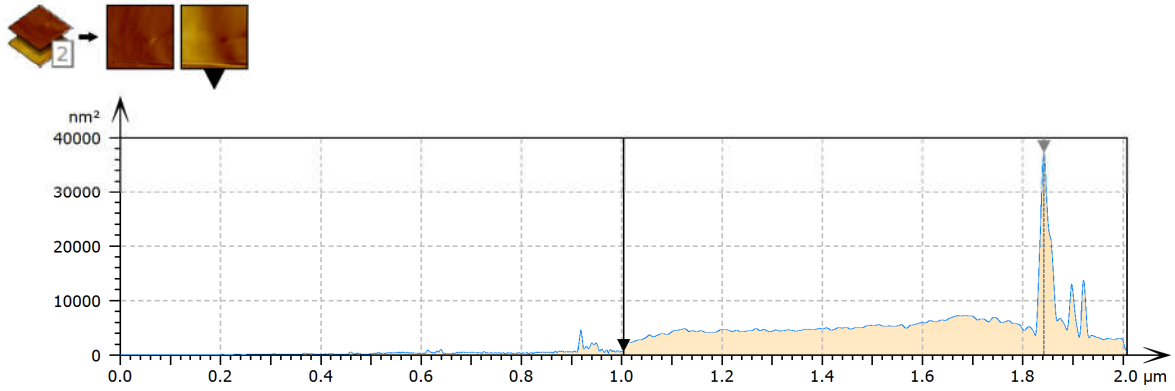

Figure 10. Spatial distribution of fibrillar orientation coherence at the mesh–tissue interface in chronic surgical mesh rejection.

Taken together, these findings suggest that the mesh–tissue interface in chronic rejection lacks a coherent structural architecture and instead exhibits a mosaic-like organization composed of independent fibrillar domains. This pattern is consistent with chronic fibro-inflammatory remodeling and impaired integration of the prosthetic material.

4. Discussion

Chronic surgical mesh rejection represents a complex pathological process characterized by persistent inflammation, foreign body reaction, and progressive extracellular matrix (ECM) remodeling [11]. The present study provides a multiscale morphological characterization of the mesh–tissue interface, showing marked structural disorganization, loss of fibrillar coherence, and pronounced surface heterogeneity.

Histological findings revealed chronic inflammatory infiltrates, increased cellularity with activated fibroblasts, and disruption of collagen architecture, consistent with previously reported features of foreign body reaction and chronic inflammatory remodeling [12]. While conventional histology provides valuable qualitative insight, it remains limited in capturing the spatial organization and nanoscale architecture of the ECM [13].

AFM analysis provided additional structural resolution, revealing pronounced topographical heterogeneity and disruption of fibrillar organization at the nanoscale [14]. The absence of coherent collagen alignment and the presence of fragmented fibrillar structures suggest that the ECM loses its capacity to maintain organized anisotropic architecture under chronic inflammatory conditions [15]. This is particularly relevant, as collagen anisotropy is essential for physiological load distribution and mechanical integrity of the abdominal wall [16].

Quantitative roughness analysis further supports advanced structural remodeling. Increased Sa and Sq values indicate surface irregularity, while elevated kurtosis (Sku) reflects isolated extreme features such as peaks and deep depressions. Negative skewness (Ssk) suggests a predominance of surface depressions, consistent with localized extracellular matrix collapse. Together, these parameters describe a highly heterogeneous surface, not consistent with normal tissue architecture [17].

Directional analysis demonstrated the absence of preferential fibrillar orientation, indicating a transition from anisotropic to near-isotropic organization. In physiological conditions, collagen alignment supports efficient force transmission [18]. The loss of directional organization observed here suggests reduced capacity of the mesh–tissue interface to respond to mechanical loading.

 doi:10.20944/preprints202604.2206.v1

Coherence mapping further demonstrated fragmentation of fibrillar architecture, with predominance of low-coherence regions and absence of extended domains of consistent orientation [19]. These findings indicate that the ECM behaves as a discontinuous structural network composed of locally independent domains, consistent with chronic fibro-inflammatory remodeling [20].

From a structural perspective, the combination of topographical heterogeneity, loss of anisotropy, and reduced coherence suggests a non-uniform distribution of mechanical loads and potential for localized stress concentration [21]. These alterations may contribute to clinical manifestations such as persistent pain, local stiffness, and functional impairment of the abdominal wall [22].

An important contribution of this study is the integration of multiple morphological descriptors, including topography, roughness, directionality, and coherence, into a unified framework for characterizing ECM disorganization. This multiscale approach highlights the importance of structural coherence as a determinant of successful implant integration.

Several limitations should be acknowledged. The relatively small sample size limits generalizability, and the analysis was restricted to morphological and nanostructural parameters without complementary mechanical testing at larger scales. In addition, AFM measurements were performed in air, which may influence absolute surface properties; however, all samples were analyzed under identical conditions, allowing reliable comparative interpretation.

Despite these limitations, the consistency of the observed structural patterns supports the relevance of nanoscale morphological analysis in understanding implant–tissue interactions.

5. Conclusions

Chronic surgical mesh rejection is associated with marked structural disorganization of the extracellular matrix at the mesh–tissue interface, characterized by loss of fibrillar coherence, absence of preferential orientation, and pronounced surface heterogeneity.

Multiscale morphological analysis using AFM suggests that the affected tissue lacks a continuous and functionally integrated architecture and instead exhibits a fragmented, mosaic-like organization composed of structurally independent domains.

These alterations are consistent with impaired tissue integration and may contribute to abnormal mechanical behavior, including non-uniform load distribution and structural instability.

The integration of nanoscale topographical, directional, and coherence analyses provides a comprehensive framework for understanding the structural basis of mesh rejection and highlights the importance of extracellular matrix organization in implant–tissue interactions.

These findings may inform future research aimed at developing improved biomaterials and surgical strategies to enhance tissue–implant compatibility and reduce the risk of chronic rejection.

Author Contributions: Conceptualization, A.T. and Ș.L.T.; methodology, A.T.; investigation, A.T., A.L., B.M.C., G.B., R.-V.L., C.S., R.D., B.F.T., and C.G.I.; data curation, A.T. and B.M.C.; formal analysis, A.T.; visualization, A.T.; writing—original draft preparation, A.T. and A.L.; writing—review and editing, A.T., A.L., B.M.C., G.B., and Ș.L.T.; supervision, Ș.L.T. All authors have read and agreed to the published version of the manuscript.

Funding: This research received no external funding.

Institutional Review Board Statement: The study was conducted in accordance with the Declaration of Helsinki and approved by the Research Ethics Committee of the "Grigore T. Popa" University of Medicine and Pharmacy, Iași, Romania (approval no. 420/31.03.2024).

Informed Consent Statement: Informed consent was obtained from all subjects involved in the study.

Data Availability Statement: The data presented in this study are available on request from the corresponding author.

Conflicts of Interest: The authors declare no conflicts of interest.

 doi:10.20944/preprints202604.2206.v1

References

1. Najm, A.; Niculescu, A.G.; Gaspar, B.S.; Grumezescu, A.M.; Beuran, M. A Review of Abdominal Meshes for Hernia Repair-Current Status and Emerging Solutions. *Materials* 2023, 16(22), 7124. https://doi.org/10.3390/ma16227124
2. See, C.W.; Kim, T.; Zhu, D. Hernia Mesh and Hernia Repair: A Review. *Eng. Regen.* 2020, 1, 19–33. HYPERLINK "https://doi.org/10.1016/j.engreg.2020.05.002"https://doi.org/10.1016/j.engreg.2020.05.002 https://doi.org/10.1172/jci.insight.123862
3. Heymann, F.; von Trotha, K.T.; Preisinger, C.; Lynen-Jansen, P.; Roeth, A.A.; Geiger, M.; et al. Polypropylene Mesh Implantation for Hernia Repair Causes Myeloid Cell-Driven Persistent Inflammation. *JCI Insight* 2019, 4(2), e123862.
4. Shiroud Heidari, B.; Dodda, J.M.; El-Khordagui, L.K.; Focarete, M.L.; Maroti, P.; Toth, L.; et al. Emerging Materials and Technologies for Advancing Bioresorbable Surgical Meshes. *Acta Biomater*. 2024, 184, 1–21. https://doi.org/10.1016/j.actbio.2024.06.012
5. Antoniadi, E.; Ferreira, N.M.; Vaz, M.F.; Parente, M.; Ferraz, M.P.; Silva, E. Innovative Strategies in Hernia Mesh Design: Materials, Mechanics, and Modeling. *Materials* 2025, 18, 3509. https://doi.org/10.3390/ma18153509 https://doi.org/10.5213/inj.1632600.318
6. Kim, Y.; Ko, H.; Kwon, I.K.; Shin, K. Extracellular Matrix Revisited: Roles in Tissue Engineering. *Int. Neurourol. J.* 2016, 20(Suppl. 1), S23–S29.
7. Marangio, A.; Biccari, A.; D'Angelo, E.; Sensi, F.; Spolverato, G.; Pucciarelli, S.; Agostini, M. The Study of the Extracellular Matrix in Chronic Inflammation: A Way to Prevent Cancer Initiation? *Cancers* 2022, 14(23), 5903. https://doi.org/10.3390/cancers14235903 https://doi.org/10.1007/s10439-019-02408-9
8. Cramer, M.C.; Badylak, S.F. Extracellular Matrix-Based Biomaterials and Their Influence upon Cell Behavior. *Ann. Biomed. Eng*. 2020, 48(7), 2132–2153.
9. Tonti, O.R.; Larson, H.; Lipp, S.N.; Luetkemeyer, C.M.; Makam, M.; Vargas, D.; Wilcox, S.M.; Calve, S. Tissue-Specific Parameters for the Design of ECM-Mimetic Biomaterials. *Acta Biomater*. 2021, 132, 4–17. https://doi.org/10.1016/j.actbio.2021.04.017 https://doi.org/10.3390/s17040938
10. Zhou, L.; Cai, M.; Tong, T.; Wang, H. Progress in the Correlative Atomic Force Microscopy and Optical Microscopy. *Sensors* 2017, 17(4), 938.
11. Ahmed, U.; Rosenberg, J.; Baker, J.J. Chronic pain and foreign body sensation based on mesh placement in primary ventral hernia repair: A systematic review highlighting the evidence gap and a call to action. *Langenbecks Arch. Surg.* 2025, 410, 132. https://doi.org/10.1007/s00423-025-03671-2
12. Mihalache, D.I.; Barbu, L.A.; Ţenea-Cojan, T.Ș.; Mărgăritescu, N.D.; Mogoantă, S.Ș.; Vasile, L.; Iordache, N. Histopathological features and tissue remodeling in chronic abdominal wall mesh infection—A clinicopathological study. *Rom. J. Morphol. Embryol.* 2025, 66, 703–709. https://doi.org/10.47162/RJME.66.4.08
13. Poole, J.J.A.; Mostaço-Guidolin, L.B. Optical microscopy and the extracellular matrix structure: A review. *Cells* 2021, 10, 1760. https://doi.org/10.3390/cells10071760
14. Joo, S.; Eom, S.; Choi, Y.; Jeong, U.; Cho, Y.; Yu, W.; Park, K.; Hong, S. Atomic force microscopy for cross-disciplinary materials research. *Small Methods* 2025, 9, e2500514. https://doi.org/10.1002/smtd.202500514
15. Junge, K.; Rosch, R.; Bialasinski, L.; et al. Persistent extracellular matrix remodelling at the interface to polymers used for hernia repair. *Eur. Surg. Res.* 2003, 35, 497–504. https://doi.org/10.1159/000073389 https://doi.org/10.1016/j.matdes.2025.114853
16. Astruc, L.; Turquier, F.; Brieu, M.; Hoc, T. Microscopic characterization of the anisotropic mechanical behavior of human linea alba and anterior rectus sheath: Contributions of collagen and elastin. *Materials & Design* 2025, 259, 114853.
17. Singh, K.; Paliwal, N.; Kasamias, K. Surface roughness characterization using representative elementary area (REA) analysis. *Sci. Rep.* 2024, 14, 1785. https://doi.org/10.1038/s41598-024-52329-4 https://doi.org/10.1016/j.actbio.2023.03.014
18. Fontenele, F.F.; Bouklas, N. Understanding the inelastic response of collagen fibrils: A viscoelastic-plastic constitutive model. *Acta Biomater.* 2023, 163, 78–90.

 doi:10.20944/preprints202604.2206.v1

19. Wang, W.Y.; Pearson, A.T.; Kutys, M.L.; Choi, C.K.; Wozniak, M.A.; Baker, B.M.; Chen, C.S. Extracellular matrix alignment dictates the organization of focal adhesions and directs uniaxial cell migration. *APL Bioeng*. 2018, 2, 046107. https://doi.org/10.1063/1.5052239
20. Diller, R.B.; Tabor, A.J. The role of the extracellular matrix (ECM) in wound healing: A review. Biomimetics 2022, 7, 87. https://doi.org/10.3390/biomimetics7030087 https://doi.org/10.1016/j.bbamcr.2015.04.006
21. Kassianidou, E.; Kumar, S. A biomechanical perspective on stress fiber structure and function. Biochim. Biophys. *Acta Mol. Cell Res*. 2015, 1853, 3065–3074.
22. Saiding, Q.; Chen, Y.; Wang, J.; Pereira, C.L.; Sarmento, B.; Cui, W.; Chen, X. Abdominal wall hernia repair: From prosthetic meshes to smart materials. *Mater. Today Bio* 2023, 21, 100691. https://doi.org/10.1016/j.mtbio.2023.100691